JOURNAL OF RESEARCH of the National Bureau of Standards — C. Engineering and Instrumentation
Vol. 71C, No. 3, July–September 1967

Torsion Creep of Circular and Noncircular Tubes*

Leonard Mordfin [1]

(March 21, 1967)

A torsion creep theory for noncircular tubes was developed by applying a multiaxial creep theory to a derived generalization of Bredt's equations.

A review of the literature revealed no torsion creep data on noncircular tubes. Hence, to evaluate the theory, a test program was carried out on twelve specimens of aluminum alloy structural tubing, of four configurations, at 400 °F.

Observed discrepancies between the torsion creep theory and experiment are smaller than variations in the measured creep properties of the specimen material from one tube configuration to another and are not appreciably greater than discrepancies between elastic torsion theory and experiment. Most of the observed discrepancies are consistent with measured anisotropy in the tubes, while other discrepancies are ascribed to nonhomogeneity in creep properties and a hydrostatic stress effect in multiaxial creep.

For the calculation of torsion stresses in circular tubes the thin-wall approximation is adequate for thickness-to-radius ratios up to one-tenth. For straight-sided tubes equivalent accuracy is obtained for effective ratios up to only one-twentieth. These criteria apply to creep conditions as well as to elastic conditions.

Key Words: Creep, primary creep, shear, shell, stress analysis, thin wall, torsion, tube.

1. Introduction

Torsion testing of thin-walled tubes furnishes a number of advantages over tensile testing in the determination of creep properties. The most significant of these is that the measurement of strain in torsion tests is essentially unaffected by the thermal expansions and contractions which accompany minor temperature fluctuations. Also, if the wall thickness is small compared to the diameter, the shear stress across the section may be regarded as uniform and, for a constant torque, this stress remains constant throughout the duration of the test. A final advantage, for certain research purposes, is that it is comparatively easy to reverse the stress direction.

In spite of these advantages most laboratory creep testing is carried out in tension. On the other hand, most structural members are subjected to multiaxial stress conditions. It is necessary, therefore, to relate creep behavior under multiaxial stress states to the uniaxial creep behavior that is usually obtained in the laboratory. The purpose of this paper is to develop a means of calculating the torsion creep behavior of noncircular tubes from the tensile creep properties of the tube materials.

The first recorded torsion creep tests of hollow tubes were carried out by Bailey [1, 2][2] in 1929. Other pioneers in this area of research include Everett [3, 4] and Lea [5]. A. E. Johnson [6–10] has probably done more work in this field than anyone else and, indeed, with the exception of one related investigation [11], Johnson was the only researcher of record engaged in torsion creep studies between 1940 and 1960. Recently, however, there has developed a mounting international interest in the subject as evidenced by the appearance of six papers [12–17] in the last three years. This is attributable, in part at least, to anticipated creep deformation problems in the wings of supersonic aircraft.

The tubular specimens used in the above investigations were, in every case, circular. This investigation is believed to be the first study of torsion creep in noncircular tubes.

Most of the torsion creep tests cited in the literature

*The results reported in this paper were used in parts of a dissertation submitted to the University of Maryland in partial fulfillment of the requirements for a Ph. D. degree. The initial phase of the work was supported by the National Aeronautics and Space Administration. An invited paper.

[1] Present address: Headquarters, Office of Aerospace Research (RROSG), 1400 Wilson Blvd., Arlington, Va. 22209.

[2] Figures in brackets indicate the literature references on page 220.

were performed on miniature test specimens having diameters of about 1/2 in and gage lengths of about 2 in. In fact, until recently [17] no torsion creep data had been reported on any tubular specimen longer than 8 in or larger than 1.6 in in diameter.

2. Theory

The theory of elastic torsion in thin-walled tubes, as developed by Bredt [18] in 1896 represents an approximation to Saint-Venant's general elastic torsion theory. Bredt's analysis was based on certain assumptions regarding the nature of the stress distribution and results in two familiar equations. The first of these, which gives the stress distribution, is

$$\tau=\frac{T}{2Ah} \tag{1}$$

where

τ = shear stress
T = torque
A = area enclosed by the midthickness curve C of the tube cross section
h = wall thickness.

This equation is derived strictly from equilibrium considerations and is, therefore, assumed to be applicable to creep conditions as well as to elastic conditions.

Bredt's second equation, which gives the angle of twist of the tube, is applicable only to elastic materials. However, a generalized version of Bredt's second equation is derived in appendix A and is applicable to material obeying any constitutive equation. This generalized version of Bredt's second equation is

$$\theta=\frac{\gamma_m P}{2A} \tag{2}$$

where

θ = angle of twist per unit length
γ_m = mean shear strain
P = perimeter of C.

It is only necessary to insert the proper expression for γ_m in this equation to make it applicable to the particular material behavior under consideration.

For the present case, let it be assumed that the tensile creep behavior of the tube material can be expressed in the common form

$$\epsilon=k\sigma^m t^n \tag{3}$$

where

ϵ = tensile creep strain
σ = uniaxial tensile stress
t = time

and k, m, and n are constants which depend only on the material and the temperature. This equation applies only to constant stress, constant temperature conditions.

If the octahedral shear stress theory of multiaxial creep is invoked, it can be shown that for a material obeying eq (3) the shear creep characteristics are given by

$$\gamma=\sqrt{3}k(\sqrt{3}\tau)^m t^n \tag{4}$$

where

γ = shear creep strain

and k, m, and n are the tensile creep constants defined by eq (3). Substituting eq (1) into eq (4) gives

$$\gamma=\sqrt{3}k\left(\frac{\sqrt{3}}{2}\frac{T}{Ah}\right)^m t^n.$$

For the case of a thin-walled tube in torsion, a mean value for the shear creep strain may be obtained by performing a contour integration of this expression around C. That is,

$$\gamma_m=\int_c \frac{\gamma ds}{P}=\sqrt{3}\frac{k}{P}\left(\frac{\sqrt{3}}{2}\frac{T}{A}\right)^m t^n\int_c \frac{ds}{h^m} \tag{5}$$

where

ds = incremental arc length of C.

Equation (5) can now be inserted into eq (2) to give the angle of twist,

$$\theta=\frac{\sqrt{3}}{2}\frac{k}{A}\left(\frac{\sqrt{3}}{2}\frac{T}{A}\right)^m t^n\int_c \frac{ds}{h^m}. \tag{6}$$

This represents the creep counterpart of Bredt's second equation. If the tube in question has a uniform wall thickness h, eq (6) simplifies to

$$\theta=\frac{\sqrt{3}}{2}\frac{P}{A}k\left(\frac{\sqrt{3}}{2}\frac{T}{Ah}\right)^m t^n. \tag{7}$$

For a circular tube with mean radius r_m this equation may be written as

$$\theta=\sqrt{3}\frac{k}{r_m}\left(\frac{\sqrt{3}}{2}\frac{T}{Ah}\right)^m t^n. \tag{8}$$

Whereas eq (7) is approximate in the sense that it was derived with Bredt's assumptions regarding the nature of the stress distribution, eq (8) is exact in the sense that it coincides with a solution (appendix B) which does not require these assumptions.

3. Test Program

A test program was designed to evaluate the applicability of eq (7) to several shapes of thin-walled tubes. Tension creep tests of the tube materials were carried out to determine k, m, and n, and torsion creep tests of the tubes were performed to provide experimental data for comparison with eq (7).

3.1. Specimens

Drawn seamless 2024–T3 aluminum alloy tubing was acquired for use as test specimens. This alloy was selected because of its reported adherence to the octahedral shear stress theory [19, 20] and because of its applicability to airframes. Four tubes of each of four different shapes were obtained: circular, square with rounded corners in two thicknesses, and rectangular with rounded corners. The diameter of the circular tubes, the sides of the square tubes, and the longer side of the rectangular tubes were all nominally 3 in, and the lengths of the tubes were each 7 ft. The nominal dimensions of the four shapes are shown in figure 1. For any single tube, variations in the outside dimensions and in the thicknesses did not exceed 0.01 in and 0.004 in, respectively.

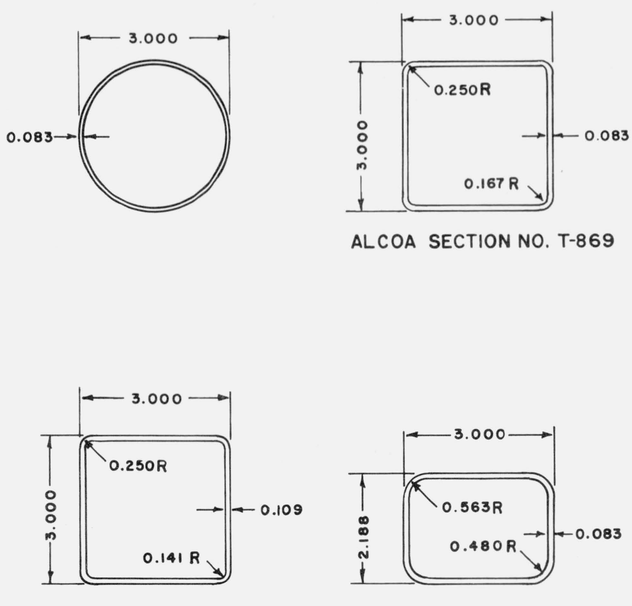

FIGURE 1. *Nominal dimensions of tube specimens, in inches.*

3.2. Tension Creep Tests

Four tension creep specimens were cut longitudinally from one tube of each of the four shapes. Using a conventional dead weight, lever arm testing machine, creep tests of approximately 50-hr duration were carried out on these specimens at 400 °F. The stress levels ranged from 9,100 to 22,500 lb/in². Using 14 data points from each test, a least squares approach was set up to find appropriate values of k, m, and n for the material of each tube shape. The resulting tension creep equations, in the form of eq (3), are as follows: For the circular tube material

$$\epsilon = 13.4\sigma^{1.05}t^{0.38} \times 10^{-6}. \tag{9a}$$

For the 0.083-in wall square tube material

$$\epsilon = 2.54\sigma^{1.60}t^{0.28} \times 10^{-6}. \tag{9b}$$

For the 0.109-in wall square tube material

$$\epsilon = 6.49\sigma^{1.33}t^{0.36} \times 10^{-6}. \tag{9c}$$

For the rectangular tube material

$$\epsilon = 2.43\sigma^{1.57}t^{0.30} \times 10^{-6}. \tag{9d}$$

In these equations σ is in kips/in² and t is in hours.

A comparison between eq (9b) and the experimental tension creep curves for the specimens cut from the 0.083-in wall square tube is given in figure 2. The discrepancies appear to be random and are attributed to the usual scatter in creep behavior. The discrepancies obtained with the specimens cut from the other tube shapes are similar to that shown in figure 2.

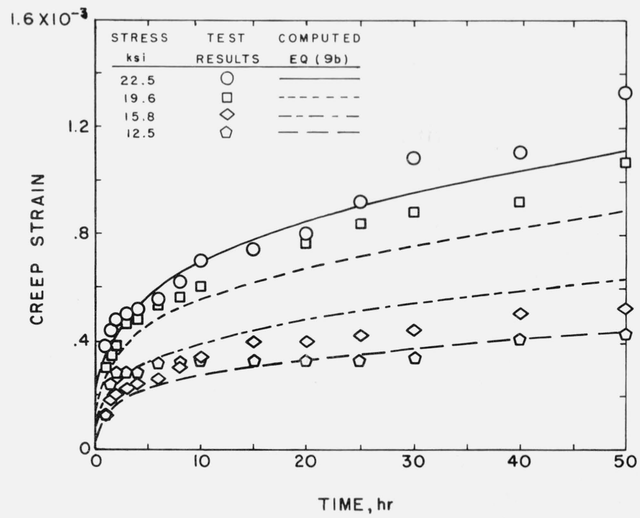

FIGURE 2. *Tension creep behavior of specimens cut from 0.083-in wall square tube.*

To compare the tensile creep properties of the four tube materials, creep curves were calculated from eqs (9) for a stress of 15,000 lb/in². These are given in figure 3. It may be seen that significant differences exist between the creep curves for the materials of two of the tube shapes as compared to those for the

265-343 O-67—3

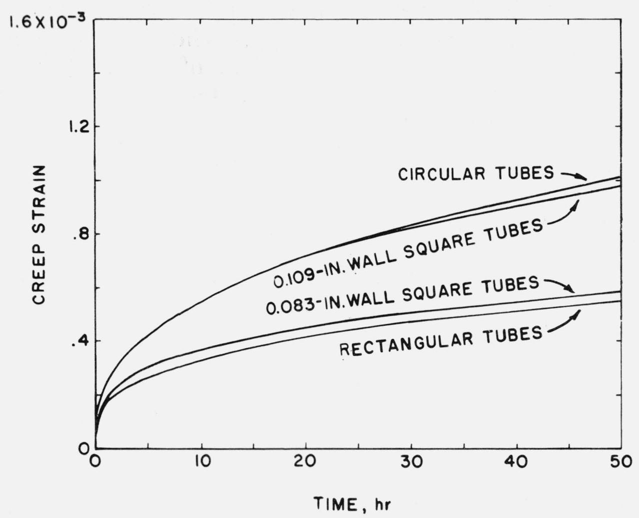

FIGURE 3. *Tension creep curves for the tube materials at 15,000 lb/in² according to eqs (9).*

materials of the other two tube shapes. These differences may be attributable to variations in chemical composition or heat treatment, or to differences in the degree of cold work resulting from the respective drawing operations.

3.3. Torsion Creep Tests

Twelve torsion creep tests were carried out at 400 °F, three on each of the four tube shapes shown in figure 1. Each tube specimen was seven feet long and was mounted such that it passed symmetrically through a six-foot test furnace. Twist measurements were made over a three-foot gage length at the center. The twist measuring system had errors not exceeding one percent and individual measurements were repeatable to better than 3×10^{-6} radians per inch. Temperatures were constant within 1 °F throughout each test and uniform, over the gage length, within 3 °F. The testing equipment, the test procedure, and the calibration technique are described in appendix C.

Table 1 lists the specimen designations, the torques, and the stress levels computed from eq (1) for each test. The experimental creep data are plotted in figures 4, 5, 6, and 7 in terms of angle of twist against time. Also given in the figures are the theoretical torsion creep curves calculated with eq (7). For the circular tubes, figure 4, and the rectangular tubes, figure 7, agreement between theory and experiment is good for the lowest stress level. At the higher stress levels the theory predicts considerably less creep than was observed in the tests. For the 0.083-in wall square tubes, figure 5, the theory predicts less creep at all stress levels than was actually obtained, while for the 0.109-in wall square tubes, figure 6, the theory predicts significantly more creep at all stress levels than was actually obtained. Although the relationship between experiment and theory is reasonably consistent for

TABLE 1. *Torsion creep tests*

Specimen No.	Torque	Shear stress	Stress error
	in-lb	*lb/in²*	*Percent*
Circular tubes			
1	9,930	8,940	+2
2	11,800	10,600	−25
3	10,900	9,820	−23
0.083-in wall square tubes			
4	11,800	8,080	−15
5	13,800	9,380	−18
6	15,600	10,700	−12
0.109-in wall square tubes			
7	16,600	8,920	+31
8	18,500	9,940	+30
9	14,700	7,900	+23
Rectangular tubes			
10	11,800	11,800	−13
11	9,350	9,350	0
12	12,800	12,800	−23

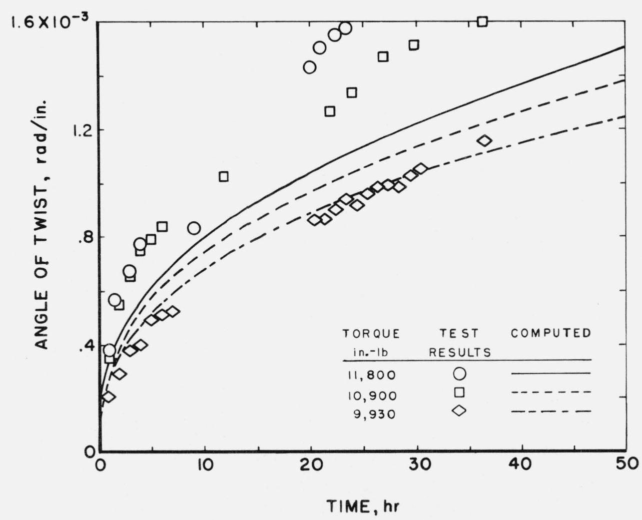

FIGURE 4. *Torsion creep behavior of circular tubes.*

each tube shape, no dominant relationship is apparent from all of the data taken together.

The discrepancies between calculated and experimental results were evaluated in terms of stress. That is, for each test the stress that would have brought the calculated curve into approximate coincidence with the experimental data was computed. The difference between this value and the theoretical stress, expressed as a percentage, is given in table 1 as the "stress error."

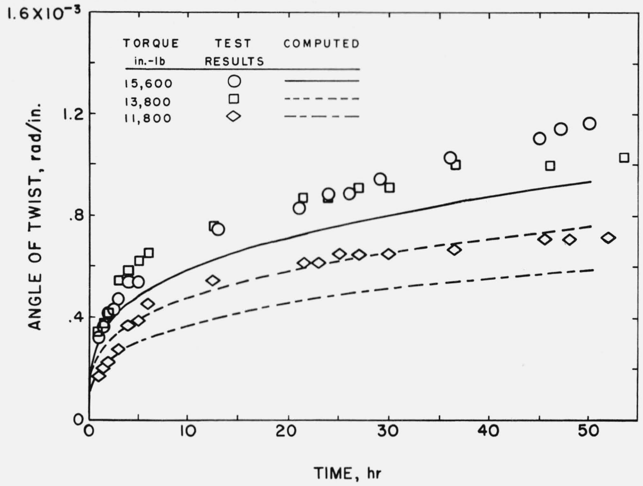

FIGURE 5. *Torsion creep behavior of 0.083-in wall square tubes.*

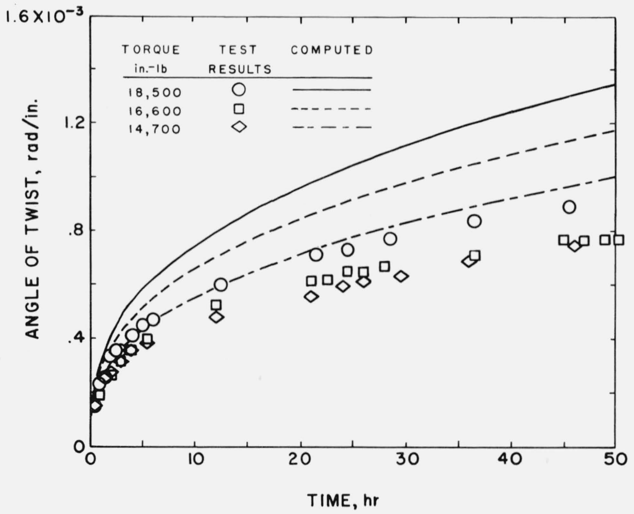

FIGURE 6. *Torsion creep behavior of 0.109-in wall square tubes.*

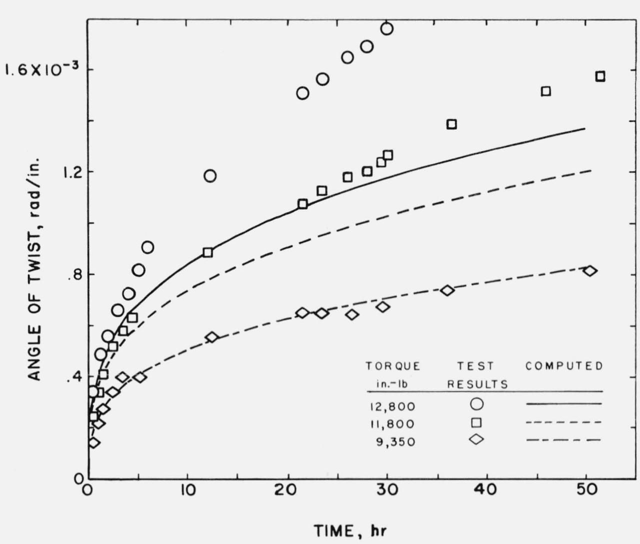

FIGURE 7. *Torsion creep behavior of rectangular tubes.*

4. Analysis of Results

The discrepancies between the theoretical and experimental creep curves are not significantly greater than the discrepancies that are obtained when Bredt's equations are applied to elastic tubes at room temperature [21–24]. This, however, does not explain the reasons for the discrepancies and, therefore, gives no indication of the limits of applicability of the theory.

In order to explain the observed discrepancies between theory and experiment, it is desirable to reexamine the justifications for the numerous assumptions which were involved in the theory. These assumptions may be divided into three categories. The first category includes those common assumptions regarding the idealization of the specimen materials which are necessary to make them amenable to mathematical treatment. These assumptions are:

1. The material is continuous.[3]
2. The material is homogeneous. (See footnote 3.)
3. The material is isotropic.

In the next category are the additional assumptions inherent in the Saint-Venant torsion theory.

4. Ends are free to extend or contract in the lengthwise direction.
5. Ends are loaded by a pure torsional couple with no resultant force.
6. There is no restraint of warping.
7. There are no reentrant corners or other areas of severe stress concentration.

Finally, there are the assumptions required by Bredt's approximation to the Saint-Venant theory.

8. The shear stress parallel to the surface is uniform throughout the wall thickness.
9. The shear stress normal to the surface is zero throughout the wall thickness.

4.1. Material Idealization

a. Continuity

Although it is known that metallic materials are composed of crystals, their dimensions are generally very small in comparison with the dimensions of the specimens. Hence, the mathematical treatment of the material as though it were continuous is generally reasonable. In the present case, however, there was some doubt as to whether the crystals were, in fact, small in comparison with the wall thicknesses of the tubes. To resolve this doubt, small samples were cut from one square tube of each of the two wall thicknesses. For each sample the number of grains in the thickness direction was counted both on a longitudinal surface and on a transverse surface. In all cases the count ranged between 33 and 48 grains. On this basis, it is felt that the assumption of continuity is justified.

[3] For these two characteristics, *continuity* and *homogeneity*, some authors prefer the terms *homogeneity* and *uniformity*, respectively. In the present context *continuity* indicates the nature of a structureless mass and *homogeneity* is the quality of having the same mechanical properties throughout the material, i.e., independent of location.

265-343 O-67—4

b. Homogeneity

It is conceivable that the tubes from which the tensile creep specimens were cut may not have been representative of the tubes which were tested in torsion creep. Therefore, the homogeneity of the specimen materials was checked, as follows, with a hardness survey.

A rectangular plate, approximately 1 in by 2 in, was cut from each torsion creep specimen, from the region which had been between the grips and the test furnace. The material in this region is considered to have suffered the least change in properties due to stressing or heating. In addition, a similar plate was cut from each of the four tubes from which the tension creep specimens had previously been cut.

Table 2 lists the average Vickers hardness numbers

TABLE 2. *Hardness test results*

Specimen No.	Hardness
	VHN
1	146
2	148
3	141
C	143
Average	144
4	147
5	148
6	145
SN	147
Average	147
7	145
8	148
9	142
SK	146
Average	145
10	145
11	140
12	141
R	140
Average	142

for each of the test plates. The plate numbers in the first column refer to the tube specimen numbers (table 1) from which the respective plates were cut. The plates designated by letter symbols refer to those tubes from which the tensile creep specimens had been cut. It can be seen that the variation in hardness within each batch is small, as expected. Unfortunately, the data also indicate that the difference in hardness from batch to batch is also small. Yet, it has been determined (fig. 3) that a significant difference in creep properties exists between different batches. Hence, it must be concluded that the uniformity in hardness within each batch does not necessarily indicate a uniformity in creep properties. The possibility thus remains that the discrepancies between the calculated and experimental torsion creep behaviors may be due to nonhomogeneity.

c. Isotropy

As a result of the cold-working process, drawn tubes are typically orthotropic with the maximum strength properties coinciding with the longitudinal direction. In the present investigation the tension creep properties of the tube materials were determined from specimens cut longitudinally from the tubes. In the torsion tests, however, the principal directions are at 45 deg to the longitudinal axis of the tubes. It is natural, therefore, to question whether the creep properties of the material in the diagonal (45-deg) direction and in the longitudinal direction are equivalent. Unfortunately, the tensile creep properties in the diagonal direction could not be evaluated in the present investigation because the specimen lengths which could be cut diagonally are too short to be satisfactorily accommodated by the available creep testing equipment.

As a compromise, it was decided to secure a general picture of the anisotropy in the tubes by conducting room-temperature tensile tests on miniature specimens which had been cut from a tube in the longitudinal, diagonal and transverse directions. The first set of miniature specimens was taken from the 0.083-in wall square tube from which the tension creep specimens had been cut. In figure 8 the longitudinal, diagonal and transverse stress-strain characteristics are compared. It may be seen that anisotropy does, indeed, exist with the material being stronger in the longitudinal direction than in the transverse direction.

Tensile and yield strengths from these tests are given in table 3, each tabulated value being the average from a pair of tests. The ratio of yield strengths

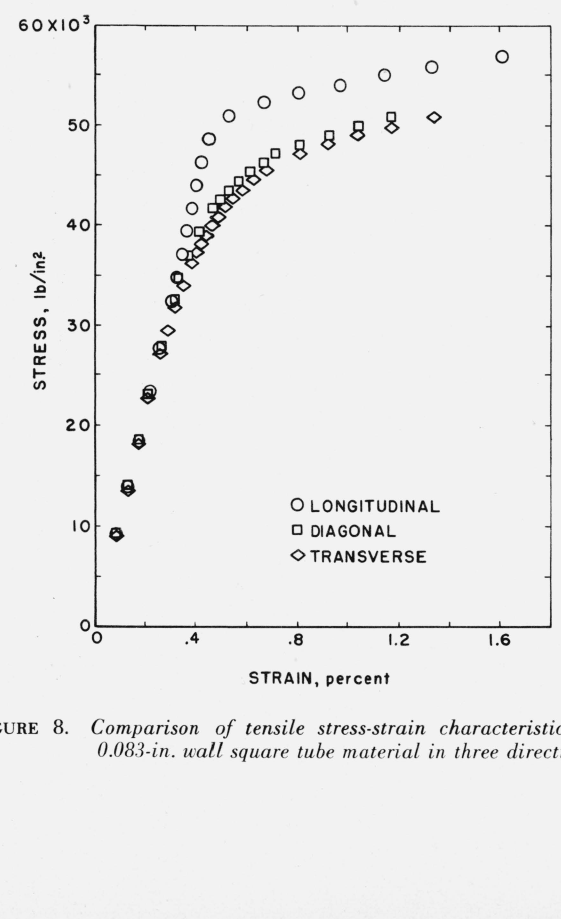

FIGURE 8. *Comparison of tensile stress-strain characteristics of 0.083-in. wall square tube material in three directions.*

TABLE 3. *Tensile properties of 0.083-in wall square tube material*

Direction	Yield strength [a]	Tensile strength
	lb/in²	*lb/in²*
Longitudinal	52,000	72,800
Diagonal	45,200	69,200
Transverse	43,500	67,800

[a] 0.2 percent offset.

in the longitudinal and diagonal directions is 1.15. If this ratio may be taken as a measure of the plastic anisotropy, then an estimate can be made of the effect of anisotropy on the torsion creep behavior of the 0.083-in wall square tubes. On the basis of this ratio it is postulated, for purposes of this estimate, that plastic flow in the diagonal direction may be deduced from the plastic flow properties in the longitudinal direction by considering the stress in the diagonal direction to be 15 percent greater than the true value. Thus, the creep strain in the diagonal direction [4] is taken as [cf eq (3)]

$$\epsilon = k(1.15\sigma)^m t^n.$$

With this modification the torsion creep equation, eq (7), becomes

$$\theta = \frac{\sqrt{3}}{2}\frac{P}{A}k\left(\frac{\sqrt{3}}{2}\frac{1.15T}{Ah}\right)^m t^n. \quad (10)$$

An independent justification for this form of anisotropy correction is given in appendix D. Torsion creep curves were calculated for the 0.083-in wall square tubes using this equation. These calculated curves are compared with the experimental results in figure 9. It is seen that, on the whole, the agreement between calculated and experimental results is now quite acceptable. The remaining discrepancies appear to be random, rather than systematic, and are apparently within the experimental variability of the creep properties of the material as exhibited by figure 2.

On similar bases it is reasonable to presume that the discrepancies obtained with the circular and rectangular tubes (figs. 4 and 7) can likewise be explained, for the most part, in terms of anisotropy. Unfortunately, however, this type of correction would increase the discrepancies obtained with the 0.109-in wall square tubes (fig. 6) since, in this case, the isotropic theory predicts considerably more creep than was observed in the tests. This situation naturally creates a suspicion that the 0.109-in wall square tubes possess a reverse type of anistropy; that is, one where the material is stronger in the diagonal (and transverse) direction than in the longitudinal direction.

[4] The degree of anisotropy is so small that the angle between the directions of principal stress and principal strain may be ignored.

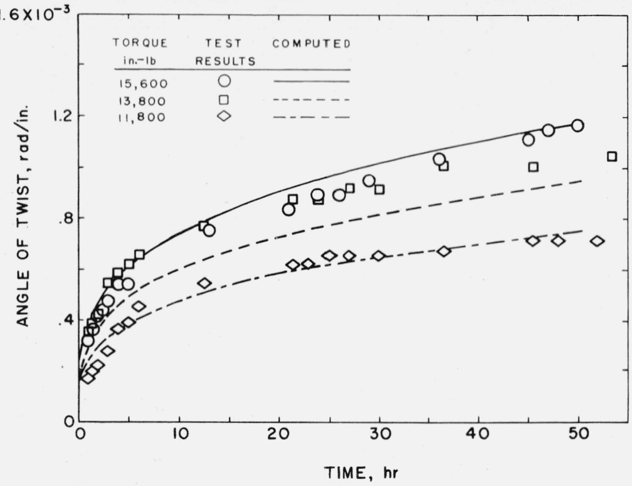

FIGURE 9. *Torsion creep behavior of 0.083-in wall square tubes.*
Comparison of experimental data with theory corrected for anisotropy.

To check this, a set of miniature specimens was cut from the 0.109-in wall square tube from which the tension creep specimens had earlier been taken. The stress-strain characteristics determined from these specimens indicate that the anisotropy in this case is qualitatively similar to that obtained with the thinner tube material (fig. 8). It must be concluded therefore, that anisotropy cannot, by itself, explain all of the discrepancies between experimental and calculated torsion creep behavior, and that some other factor or factors, as yet unknown, are operative here.

The tensile and yield strengths for the 0.109-in wall square tube material are given in table 4.

TABLE 4. *Tensile properties of 0.109-in wall square tube material*

Direction	Yield strength [a]	Tensile strength
	lb/in²	*lb/in²*
Longitudinal	55,700	70,900
Diagonal	47,200	69,600
Transverse	43,300	67,500

[a] 0.2 percent offset.

d. Compressive Creep Properties

Another assumption of concern here, which is related to the matter of isotropy, is the equivalence of the creep properties in tension and in compression. This was not listed as a separate assumption but it is inherent in the octahedral shear stress theory of multiaxial creep, which was used in the development of the torsion creep equations. Vawter et al. [25], and Heimerl and Farquhar [26] measured and compared the tensile and compressive creep properties of 2024–T3 aluminum alloy at several temperatures. Although no data were obtained at 400° F their results suggest that at this temperature the creep properties in tension and compression are probably close to one another. Similar results have been reported [27] for 2024–T4 aluminum alloy.

4.2. End Effects

Assumptions 4, 5, and 6 may be considered collectively under the heading of end effects. Conformance with these three assumptions is required in order to achieve, in the specimen, the state of pure torsional loading which is considered in the theory.

a. Longitudinal Restraint

If a tubular specimen were to manifest a tendency to lengthen or shorten under torsion, and if this tendency were resisted, axial stresses would be induced in the tube. Accordingly, the design of the torsion creep testing equipment incorporated provision for the torquing shaft to slide axially in its bearings. Thus, with exception of some friction, the torqued end of the specimen was free to extend or contract.

b. Applied Stress Distribution

The Saint-Venant solution to the torsion problem concludes that the stress distribution is the same at every cross section. This indicates that, for conformance with the theory, the torque must be applied to the end surface of the cylinder as a system of tractions identical with the shear stress distribution which is thence obtained at every cross section. The restrictive nature of this requirement is eased by the application of Saint-Venant's principle, which is usually satisfactory. In the case of thin-walled members, however, it has been known for some time that Saint-Venant's principle is not universally valid.

With a thin-walled tube in torsion, if the applied system of shear forces is not identical with the derived shear stress distribution, then longitudinal normal stresses are created in order to maintain compatability of the deformation at the ends. (This is illustrated later for the case of a square tube.) These normal stresses differ from those induced by the restraint of elongation or contraction in that they are self-equilibrating at any cross section. Nevertheless, these stresses may make themselves felt at longitudinal distances which are many times the depth or diameter of the tube.

Thus, assumption No. 5, which is adequate for solid cylinders is inadequate for thin-walled tubes. Instead, strict conformance with the Saint-Venant torsion theory requires that the torque be applied in such a way that the applied distribution of shear forces is identical with the derived distribution of shear stresses. In a practical sense, deviations can be tolerated only if the induced longitudinal stresses are comparatively small.

The dissipation of the longitudinal normal stresses with distance from the ends was calculated by Vlasov's method [28] for the square and rectangular tubes of the present investigation. The results of the calculations are given in figure 10, which shows the variation

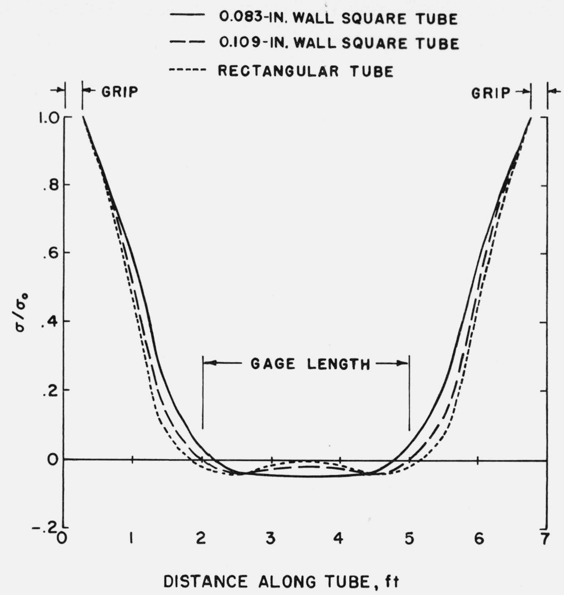

FIGURE 10. *Dissipation of longitudinal normal stresses.*

of the longitudinal normal stresses σ as a fraction of the indeterminate value σ_0 at the ends. It may be seen that, owing to the fact that 21-in lengths of tube were provided between the grips and the gage length, the longitudinal stresses within the gage length have dissipated to less than five percent of the values at the ends of the tubes. This indicates that the conversion of the applied shear stress distribution into the Saint-Venant shear stress distribution is essentially accomplished. Only in an infinitely long tube would this conversion be complete.

The absence of significant longitudinal normal stresses within the gage length was checked experimentally with strain gages, as described in appendix C.

c. Warping

In the case of rectangular tubes, longitudinal normal stresses are also introduced by the restraint of warping. The effects of these stresses on torsional stiffness were calculated by von Kármán and Chien [29]. From their results it was determined that, for the rectangular tubes tested in the present investigation, the restrained warping causes a noticeable effect on the angle of twist for distances of only an inch or two from the grips. Thus, within the gage length, the warping may be considered to be unrestrained, as required by assumption No. 6.

4.3. Stress Concentration

The square and rectangular tubes used in the present investigation were selected with rounded corners in order to minimize the stress concentrations. These stress concentrations were evaluated from Huth's charts [30] as follows:

For the 0.083-in wall square tubes, $k_c = 1.02$;
for the 0.109-in wall square tubes, $k_c = 1.15$;
for the rectangular tubes, $k_c = 1.00$.

It may be seen that the stress concentrations are, indeed, small. The largest value, for the 0.109-in wall square tubes, cannot reasonably explain the discrepancies observed between the theoretical and experimental torsion creep results. If anything, the stress concentration would tend to cause greater experimental deformations than the theory predicts whereas, in fact, the opposite was observed with the 0.109-in wall square tubes.

4.4. Thickness Effects

Assumptions 8 and 9, which are required by Bredt's analysis, may be discussed under the subject of thickness effects since, to a large extent, these assumptions are justified if the wall thickness is small enough.

a. Stress Gradient

Curiously, there is no well-known criterion or rule-of-thumb which defines the maximum thickness or other limiting condition for application of thin-wall torsion theory. On the other hand, for pressure vessels there is a widely quoted criterion that defines a thin cylinder as one in which the wall thickness is less than one-tenth of the radius. It is interesting to examine this criterion with a view toward establishing a similar one for torsion.

(1) *Circular Tubes.* In an internally pressurized circular tube the tangential stresses vary through the wall thickness, reaching a maximum at the inside surface. Under elastic conditions the maximum stress, as given by Lame's equation, may be written as

$$\sigma_{\max}=p\left(\frac{1}{\alpha}+\frac{\alpha}{4}\right)$$

where p is the pressure and α is the ratio of the wall thickness h to the mean radius r_m. For thin-walled tubes the tangential stress is considered to be uniform through the thickness with a value of

$$\sigma_{\text{thin}}=\frac{pr_i}{h}=p\left(\frac{1}{\alpha}-\frac{1}{2}\right)$$

where r_i is the inside radius. The ratio

$$\frac{\sigma_{\max}}{\sigma_{\text{thin}}}=\frac{\frac{1}{\alpha}+\frac{\alpha}{4}}{\frac{1}{\alpha}-\frac{1}{2}} \tag{11}$$

is an index of the error of the thin-wall approximation for any specific value of α.

For elastic torsion of a circular tube the shear stresses vary through the thickness, reaching a maximum at the outside surface. The maximum stress, as given by Saint-Venant's theory, may be written as

$$\tau_{\max}=\frac{T}{4\pi r_m^3}\,\frac{1+\frac{\alpha}{2}}{\frac{\alpha}{2}+\frac{\alpha^3}{8}}$$

where T is the torque. For thin tubes the shear stress is considered to be uniform through the thickness with a value

$$\tau_{\text{thin}}=\frac{T}{2Ah}=\frac{T}{2\pi r_m^3}\left(\frac{1}{\alpha}\right).$$

The ratio of the maximum shear stress to the shear stress given by the thin-wall theory is

$$\frac{\tau_{\max}}{\tau_{\text{thin}}}=\frac{1+\frac{\alpha}{2}}{1+\frac{\alpha^2}{4}}. \tag{12}$$

Equations (11) and (12) are plotted in figure 11. It is seen that the error involved in the thin-wall approximations is greater for the pressure case than for the torsion case. Hence, a criterion applicable to the pressure case is reasonable for the torsion case as well. When $\alpha=0.1$ the error is slightly more than five percent for the pressure case and slightly less than five percent for the torsion case. For the circular tubes tested in the present investigation, $\alpha=0.057$, which corresponds to an error of less than three percent.

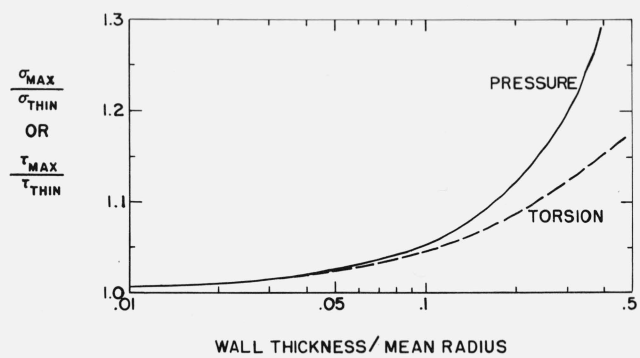

FIGURE 11. *Effect of wall thickness on the thin-wall approximation of the stress.*

(2) *Straight-Sided Tubes.* For elastic torsion of square or rectangular tubes the situation is not as favorable. If a mean radius for straight-sided tubes is defined by

$$r_m=\frac{2A}{P} \tag{13}$$

and if the stress concentrations at the corners are neglected, then the maximum shear stress at the outer surface is [24, 31]

$$\tau_{\max}=\frac{T}{2Ah}\ (1+\alpha).$$

Therefore,

$$\frac{\tau_{\max}}{\tau_{\text{thin}}}=1+\alpha.$$

Using the criterion of five percent error that was used above it appears that, for straight-sided tubes in torsion, thin-wall theory is applicable only if α is less than 0.05, rather than 0.1, which is the case for circular tubes. The following values of α apply to the square and rectangular tubes tested in the present investigation:

For the 0.083-in wall square tubes, $\alpha=0.057$;
for the 0.109-in wall square tubes, $\alpha=0.074$;
for the rectangular tubes, $\alpha=0.066$.

Clearly, the wall thicknesses for these tubes exceed the limit within which thin-wall torsion theory is accurate. However, this limit applies only to the stresses. It has been shown [32, 33] that the thin-wall requirement is far less restrictive for the calculation of angle of twist than it is for the calculation of stresses. Hence, the use of the thin-wall approach is acceptable for present purposes.

(3) *Effect of Creep.* For the case of circular tubes the exact creep stress distribution is given by eq (B.3) in appendix B. As an illustration of this stress distribution, this equation, with $r_m=1$ and $h=0.1$, is plotted in figure 12 for creep exponents of $m=1$, $m=2$, and $m=\infty$. The curve for $m=1$ represents the elastic stress distribution. The curve for $m=2$ represents a creep stress distribution where elastic strains are negligible in comparison with the creep strains. For a real case where a combination of elastic and creep strains exist the distribution would lie somewhere between the curves for $m=1$ and $m=2$. The curve for $m=\infty$ represents the uniform stress distribution assumed by Bredt's thin-wall theory. Thus, it is seen that in creep the stress distribution is actually closer to the thin-wall approximation than it is under elastic conditions. It may be concluded, therefore, that any criterion which defines a limiting wall thickness for elastic torsion is acceptable for creep conditions, too.

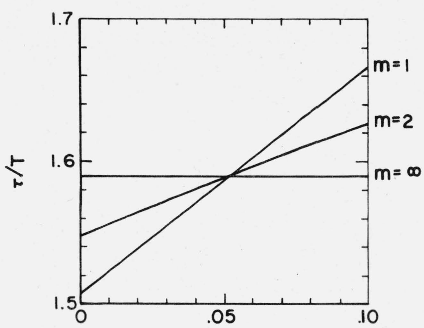

FIGURE 12. *Variation of shear stress through the wall of a circular tube in torsion.*

b. Stress Direction

Assumption No. 9 requires that all shear stresses be parallel to the surface of the tube. Thinking in terms of the hydrodynamic analogy, this appears to be a reasonable assumption for tubes of smooth contour, such as circles, but it can be demonstrated that it is somewhat erroneous for tubes with corners.

Consider, for example, torsion of a thin-walled tube of length L having a cross section in the form of a square with sides of length u and thickness h. This is shown diagramatically in two views in figure 13(a). According to the assumption, the shear stresses τ in each side of the square are parallel to the surface. If these are considered to be the only stresses acting, the only deformation which could take place is pure shear with displacements δ as shown in figure 13(b). (Only one face is shown in the left view, for simplicity. The broken lines indicate the original, undeformed shape.) The angle γ is simply the shear strain τ/G', where G is the modulus of rigidity and the prime is added for generality; G' and γ may be considered time-dependent to allow for creep. Displacement δ is equal to γL.

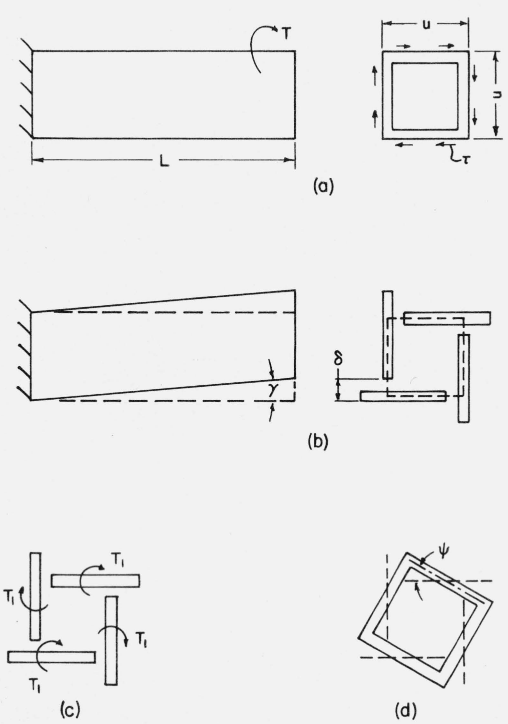

FIGURE 13. *Deformation of a square tube in torsion.*

This deformation pattern is clearly unacceptable by itself. What is required to restore compatability to the tube shape is a torsion of each face about its own longitudinal axis, as indicated by the torques T_1 in figure 13(c). The final configuration is shown in figure 13(d), where the required angle of twist is

$$\psi=\frac{2\delta}{u}=\frac{2\gamma L}{u}=\frac{2\tau L}{G'u}.$$

The torques T_1 are comprised of shear stresses near the corners which act normal to the surface although they are necessarily zero at the surface. The magnitude of T_1 is simply the torque required to twist a flat strip through angle ψ. That is,

$$T_1=\left(\frac{\psi}{L}\right)JG'=\frac{2\tau}{G'u}\frac{uh^3}{3}G'=\frac{2}{3}\tau h^3$$

where J is the torsional constant.

The condition of moment equilibrium can now be imposed. The four torques T_1 plus the moment of the shear stresses τ [fig. 13(a)] must equal the applied torque T. That is,

$$T=4T_1+4(\tau hu)\frac{u}{2}=\frac{8}{3}\tau h^3+2\tau hu^2$$

from which

$$\tau=\frac{T}{2h\left(\frac{4}{3}h^2+u^2\right)}.$$

According to Bredt's equation, however, the shear stress is

$$\tau=\frac{T}{2Ah}=\frac{T}{2hu^2}.$$

The difference, expressed as a fraction of the Bredt stress is

$$\frac{\Delta\tau}{\tau}=\frac{1}{1+\frac{3u^2}{4h^2}}.$$

This quantity is negligible for the square tubes tested in the present investigation and, in fact, amounts to less than one percent for h/u ratios up to one-tenth.

The presence of shear stresses normal to the surface of the tube introduces another source of error, namely, distortion of the cross-sectional shape in its own plane. This distortion changes the enclosed area and, therefore, the stresses as well. This problem was studied in detail by Ikeda [34] for square, thin-walled tubes. Using the results of his analysis it was determined that the effect on the stresses is less than one percent for the square tubes tested in the present investigation.

5. Discussion

The foregoing analyses have demonstrated that the assumptions introduced by Bredt's approximation to the Saint-Venant torsion theory are applicable to the torsion creep problem studied in this investigation. In the area of material idealization, however, some aspects of questionable applicability were revealed. Specifically, it was found that the materials of the tubes tested were not isotropic. However, with an approximate correction for anisotropy, satisfactory coincidence between theory and experiment was shown to be attainable. Unfortunately, this was not the case for the 0.109-in wall square tubes.

The studies carried out were inadequate to demonstrate that the specimen materials are homogeneous insofar as creep properties are concerned. Therefore, the discrepancies between theory and experiment could logically—although tentatively—be ascribed to nonhomogeneity; little can be done with such a problem unless the actual distribution of creep properties in the specimen is known. Intuitively, however, this is an unsatisfactory conclusion. The discrepancies (fig. 6) appear too large and too consistent to be attributed to a negative characteristic such as an absence of homogeneity. The fact that the discrepancies are not appreciably greater than those obtained under elastic conditions does not mitigate the need for a more satisfactory explanation, and at least one other possible explanation does exist.

In the preceding sections most of the assumptions involved in the development of the theory were justified or evaluated by measurements or calculations applicable to the problem at hand. The justifications for two of the assumptions, however, were based on references to data in the literature. These two assumptions, which are related, are the octahedral shear stress theory of multiaxial creep, and the equivalence of tensile and compressive creep. The failure of the torsion creep theory to describe the behavior of the 0.109-in wall square tubes is reason enough to reexamine the adequacy of these justifications. Although the octahedral shear stress theory is reported to be the one most commonly used at the present time [35] and also most favored by the weight of evidence in the literature [36], careful experimental measurements have been presented, in recent years, which are inconsistent with it [12, 37].

Some investigators are inclined to the belief that inconsistencies with the octahedral shear stress theory are somehow attributable to an effect of hydrostatic stress. The theory neglects such an effect but a difference between tensile and compressive creep properties would indicate that the effect is not negligible. Finnie [12] attempted to evaluate this effect experimentally and found that it could not be characterized by any simple modification of the octahedral shear stress theory. By means of a literature search, he also concluded that the hydrostatic stress effect becomes significant only when the absolute test temperature exceeds half the absolute melting temperature of the test material, and proposes this as an explanation for the belief (which was widespread until recently) that the hydrostatic stress effect is negligible. In this context it is significant that the tests in the present investigation were conducted at a temperature which does, in fact, exceed half the absolute melting temperature of the specimen material.

The current state of knowledge regarding creep under multiaxial stresses was adequately summed up by Manson [35] in his discussion of the octahedral shear stress formulation:

> Whether the quantitative discrepancies that occur . . . are due to the inadequacy of the formulation still remains to be established. If modifications are to be made, the question must still be resolved as to whether they should be in the form proposed by Wahl [38], or by a suitable correction which includes hydrostatic stress, or whether still another interpretation is best.

It appears that an improved torsion creep theory for noncircular tubes must await the development of an improved multiaxial creep theory.

6. Conclusions

A theory for the torsion creep behavior of thin-walled tubes was developed by applying the octahedral shear stress theory of multiaxial creep to a generalized version of Bredt's equations. The theory was compared with experimental results obtained by tests on 12 large circular and noncircular aluminum alloy tubes at 400 °F. The following principal conclusions, applicable to the material and tube configurations tested herein, were obtained:

1. In most cases the theory can provide usable results when suitable allowances or corrections are made for anisotropy.

2. Aside from the effects of anisotropy, differences between theory and experiment have been tentatively ascribed to (a) a shortcoming in existing theory of multiaxial creep behavior which is related to the inequality of tensile and compressive creep properties, or (b) nonhomogeneity in creep properties.

3. The largest differences between theory and experiment were obtained with the 0.109-in wall square tubes. These differences were conservative and are smaller than the differences in the measured creep properties of the material from batch to batch. Also, the differences between theory and experiment are not appreciably larger than the discrepancies obtained when Bredt's equations are used to predict the torsion behavior of elastic tubes at room temperature.

Other conclusions of interest which were obtained in the course of the investigation are:

1. The existence of nonhomogeneity in creep properties at elevated temperatures is not, necessarily, revealed by measurements of other mechanical properties at room temperature.

2. For the calculation of stresses in circular tubes the thin-wall approximation may be considered adequate for thickness-to-radius ratios up to one-tenth. For straight-sided tubes equivalent accuracy is obtained for ratios up to only one-twentieth, where the effective radius is defined as in eq (13). These criteria are applicable under creep conditions as well as under elastic conditions. For the calculation of twist angles the thin-wall approximation presumably is less restrictive than it is for the calculation of stresses.

3. A simple and unique analysis is presented for evaluating the shear stresses which act normal to the surface of square tubes under torsion. It is shown that the effect of these stresses, on the overall stress distribution, is negligible for thin-walled tubes.

7. References

[1] R. W. Bailey, Creep of steel under simple and compound stresses and the use of high initial temperature in steam power plant, Trans. Tokyo Sectional Meeting, World Power Conf. **3**, 1089 (1929).

[2] R. W. Bailey, The utilization of creep test data in engineering design, Proc. Inst. Mech. Eng. **131**, 131 (1935).

[3] F. L. Everett, Strength of materials subjected to shear at high temperatures, Trans. Am. Soc. Mech. Eng. **53**, 117 (1931).

[4] F. L. Everett and C. L. Clark, Report on torsion creep tests for comparison with tension creep tests on a carbon-molybdenum steel, Proc. Am. Soc. Testing Materials **39**, 215 (1939).

[5] F. C. Lea, discussion of [2], Proc. Inst. Mech. Eng. **131**, 334 (1935).

[6] H. J. Tapsell and A. E. Johnson, Creep under combined tension and torsion, part 1, the behavior of a 0.17 percent carbon steel at 455 deg C., Engineering (London) **150**, 24 (1940).

[7] A. E. Johnson, Behavior of cast steel at elevated temperatures, Engineer (London) **188**, 126 (1949).

[8] A. E. Johnson, The creep of a nominally isotropic aluminum alloy under combined stress systems at elevated temperatures, Metallurgia (Manchester) **40**, 125 (1949).

[9] A. E. Johnson, The creep of a nominally isotropic magnesium alloy at normal and elevated temperatures under complex stress systems, Metallurgia (Manchester) **42**, 249 (1950).

[10] A. E. Johnson, Creep under complex stress systems at elevated temperatures, Proc. Inst. Mech. Eng. **164**, 432 (1951).

[11] G. Gerard and A. C. Gilbert, A critical strain approach to creep buckling of plates and shells, J. Aero/Space Sci. **25**, 429 (1958).

[12] I. Finnie, An experimental study of multiaxial creep in tubes, Proc. Joint Intern. Conf. on Creep, p. 2/21 (Inst. Mech. Eng., London, 1963).

[13] J. L. Gubser, O. M. Sidebottom and M. R. Shammamy, Creep torsion of prismatic bars, Proc. Joint Intern. Conf. on Creep, p. 2/99 (Inst. Mech. Eng., London, 1963).

[14] V. P. Sdobyrev, Creep and durable strength under combined tensile and torsional stress, Engineering J., No. 2, p. 391 (NBS Joint Publ. Research Service, 1963). Translated from Inzhenernyy Zhurnal (Moscow) **3**, 413 (1963).

[15] S. Taira, R. Koterazawa and R. Mamiya, Creep under the changing combined tension-torsion stress system, Proc. 7th Jap. Cong. Testing Materials, p. 56 (1964).

[16] N. R. Bauld, Jr., and O. M. Sidebottom, Experimental and theoretical evaluation of several creep theories for creep torsion of circular bars, Developments in Theoretical and Applied Mechanics **2**, 557 (1965).

[17] E. Z. Stowell and R. K. Gregory, Steady-state biaxial creep, Trans. Am. Soc. Mech. Eng. [E] **32**, 37 (1965).

[18] R. Bredt, Critical observations on elastic torsion (in German), Z. Ver. Deut. Ingenieure **40**, 785 (1896).

[19] G. I. Taylor and H. Quinney, The plastic distortion of metals, Trans. Roy. Soc. London [A] **230**, 323 (1931).

[20] W. T. Lankford, J. R. Low and M. Gensamer, The plastic flow of aluminum alloy sheet under combined loads, Trans. Am. Inst. Mining Met. Eng. **171**, 574 (1947).
[21] P. Kuhn, The torsional stiffness of thin duralumin shells subjected to large torques, NACA TN 500 (1934).
[22] W. Hovgaard, Torsion of rectangular tubes, J. Applied Mech. **4**, A131 (1937).
[23] S. Levy, A. E. McPherson and W. Ramberg, Torsion test of a monocoque box, NACA TN 872 (1942).
[24] R. L. Moore and D. A. Paul, Torsion tests of 24S-T aluminum-alloy noncircular bar and tubing, NACA TN 885 (1943).
[25] F. J. Vawter, G. J. Guarnieri, L. A. Yerkovich and G. Derrick, Investigation of the compressive, bearing, and shear creep-rupture properties of aircraft structural metals and joints at elevated temperatures, Wright Air Development Center Tech. Rep. 54–270, Part 2 (1956).
[26] G. J. Heimerl and J. Farquhar, Compressive and tensile creep of 7075–T6 and 2024–T3 aluminum-alloy sheet, NASA TN D–160 (1959).
[27] O. K. Salmassy, R. J. MacDonald, R. L. Carlson and G. K. Manning, An investigation of the interchange of tensile creep for compressive creep, part 1, types 2024–T4 and 1100–0 aluminum, Wright Air Development Center Tech. Rep. 56–26, Part 1 (1956).
[28] V. Z. Vlasov, Thin-walled elastic beams, 2d ed., pp. 244–249 (Israel Program for Scientific Translations, Jerusalem, 1961). Translation of Tonkostennye uprugie sterzhni (Gosudarstvennoe izdatelstvo fiziko-matematicheskoi literatury, Moscow, 1959).
[29] T. von Kármán and W. Z. Chien, Torsion with variable twist, J. Aeron. Sci. **13**, 503 (1946).
[30] T. H. Huth, Torsional stress concentration in angle and square tube fillets, J. Applied Mech. **17**, 388 (1950).
[31] D. Williams and J. Taylor, Variations of shear stress in thin-walled tubes under torque, Aeron. Research Comm. (London) Rep. & Mem. No. 1812 (1938).
[32] P. Kuhn, Stresses in aircraft and shell structures, p. 14 (McGraw-Hill Book Co., Inc., New York, 1956).
[33] R. M. Koper, Twist and shear in thin-walled bars under torsion, Product Eng. **34**, No. 22, 92 (Oct. 28, 1963).
[34] K. Ikeda, Failure of non-circular thin tubes in torsion, calculations and experiments about square thin tubes (in Japanese with English abstract), J. Soc. Aeron. Sci. Nip. **7**, 426 (1940).
[35] S. S. Manson, Design considerations for long life at elevated temperatures, Proc. Joint Intern. Conf. on Creep **2**, D29 (Inst. Mech. Eng., London, 1965).
[36] G. H. Rowe, J. R. Stewart and K. N. Burgess, Capped end, thin-wall tube creep-rupture behavior for type 316 stainless steel, Trans. Am. Soc. Mech. Eng. [D] **85**, 71 (1963).
[37] A. M. Wahl, G. O. Sankey, M. J. Manjoine and E. Shoemaker, Creep tests of rotating disks at elevated temperature and comparison with theory, Trans. Am. Soc. Mech. Eng. **76**, 225 (1954).
[38] A. M. Wahl, Application of the modified Bailey equations for creep under biaxial tension stress, Proc. 4th U.S. Nat. Cong. Applied Mech., p. 1167 (Am. Soc. Mech. Eng., 1962).
[39] I. Finnie and W. R. Heller, Creep of engineering materials, pp. 147–148 (McGraw-Hill Book Co., Inc., New York, 1959).
[40] L. M. Kachanov, Theory of creep (in Russian), p. 90 (Fizmatgiz, Moscow, 1960).

Appendix A. Generalized Version of Bredt's Second Equation

Consider a cylindrical shell of closed section having a length L and faces normal to the cylinder axis. See figure 14. Under an applied torque T an originally longitudinal element AB of the midsurface rotates to an orientation AB'. Angle BAB' is the shear strain γ. Displacement $\overline{BB'}$ is equal to $L\gamma$ and it is assumed that the strains are sufficiently small that this displacement is perpendicular to the radius r from the axis of torsion.

The angle of twist, viewed from this axis, is

$$\psi=\frac{\overline{BB'}}{r}=\frac{L\gamma}{r} \tag{A.1}$$

and the angle of twist per unit length is

$$\theta=\frac{\psi}{L}=\frac{\gamma}{r}. \tag{A.2}$$

It is clear that this quantity does not remain constant as midthickness curve C is traversed. Yet it is common and desirable to assign a single value to the quantity known as angle of twist per unit length. Generally, this question is ignored and θ is computed either by the membrane analogy or by a strain energy approach, both of which yield an effective mean value θ. A mean value is also sought here, but the membrane analogy and the strain energy method will not be used since these approaches apply principally to elastic materials.

A mean radius can be deduced from the relation

$$r_m=\frac{2A}{P} \tag{A.3}$$

where P is the perimeter of C and A is its enclosed

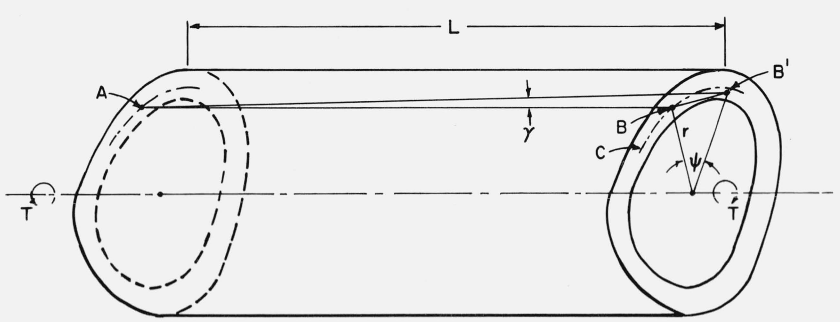

FIGURE 14. *Derivation of generalized version of Bredt's second equation.*

area. Then, designating the mean shear strain as γ_m leads to the following expression for angle of twist.

$$\theta = \frac{\gamma_m}{r_m} = \frac{\gamma_m P}{2A}. \tag{A.4}$$

This equation may be regarded as a generalized version of Bredt's second equation.

Appendix B. Torsion Creep of Circular Tube

Consider a hollow circular rod in torsion with inside radius a and outside radius b. The shear creep properties of the material are given by eq (4). Then, neglecting elastic strains for the moment,[5] the shear stress at any radius r is shown [39, 40] to be

$$\tau = \frac{\left(3+\frac{1}{m}\right)T}{2\pi b^3\left[1-\left(\frac{a}{b}\right)^3+\frac{1}{m}\right]}\left(\frac{r}{b}\right)^{1/m}. \tag{B.1}$$

The shear strain distribution is obtained by substituting eq (B.1) into eq (4), giving

$$\gamma = \sqrt{3}\,k\,\frac{r}{b}\left[\frac{\sqrt{3}\left(3+\frac{1}{m}\right)T}{2\pi b^3\left[1-\left(\frac{a}{b}\right)^{3+1/m}\right]}\right]^m t^n.$$

Then the angle of twist is

$$\theta = \frac{\gamma}{r} = \frac{\sqrt{3}\,k}{b}\left[\frac{\sqrt{3}\left(3+\frac{1}{m}\right)T}{2\pi b^3\left[1-\left(\frac{a}{b}\right)^{3+1/m}\right]}\right]^m t^n. \tag{B.2}$$

For a thin-walled circular tube let the mean radius be r_m and the wall thickness be h so

$$b = r_m + \frac{h}{2} \text{ and } a = r_m - \frac{h}{2}.$$

Then the stress distribution, eq (B.1), becomes

$$\tau = \frac{\left(3+\frac{1}{m}\right)T}{2\pi r_m^3\left[\left(1+\frac{h}{2r_m}\right)^{3+1/m}-\left(1-\frac{h}{2r_m}\right)^{3+1/m}\right]}\left(\frac{r}{r_m}\right)^{1/m}. \tag{B.3}$$

Since $\frac{h}{2r_m} \ll 1$, the quantity in brackets in the denominator reduces to approximately $2\left(3+\frac{1}{m}\right)\frac{h}{2r_m}$. Thus, the stress distribution may be written as

$$\tau = \frac{T}{2\pi r_m^2 h}\left(\frac{r}{r_m}\right)^{1/m}. \tag{B.4}$$

[5] The effect of the elastic component is discussed in section 4.4a(3).

Using a similar approach, the angle of twist, eq (B.2), may be rewritten as

$$\theta = \frac{\sqrt{3}k}{r_m}\left(\frac{\sqrt{3}T}{2\pi r_m^2 h}\right)^m t^n$$

or

$$\theta = \frac{\sqrt{3}k}{r_m}\left(\frac{\sqrt{3}T}{2Ah}\right)^m t^n. \tag{B.5}$$

This is identical with eq (8) which was derived with the generalized Bredt equation. Note also that the shear stress at the mean radius, from eq (B.4), is

$$\tau_m = \frac{T}{2\pi r_m^2 h} = \frac{T}{2Ah}$$

which is the value of the uniform shear stress according to Bredt's first equation.

Appendix C. Details of Torsion Creep Tests

C.1. Equipment

An overall view of the torsion creep testing equipment is shown in figure 15. Close-up views of the left and right ends of the setup are given in figures 16 and 17, respectively.

The ends of the specimen (A, figs. 15 and 16) are reinforced with close-fitting plugs to a depth of three inches. The specimen is mounted such that it passes through the test furnace (B, figs. 15, 16 and 17). The plugged left end of the specimen is rigidly bolted to a welded lug on a building column. The right end of the specimen is fastened, by means of a keyed shaft passing through the end plug, to a large sprocket wheel (C, figs. 15, 16 and 17). The shaft is supported by three journal bearings used at only a small fraction of their load capacity. The horizontal positions of the bearings are adjustable, both longitudinally and laterally, to permit proper alinement of the shaft with the fixed end mounting. The sprocket wheel, which has a pitch diameter of 38.2 in, applies torque to the

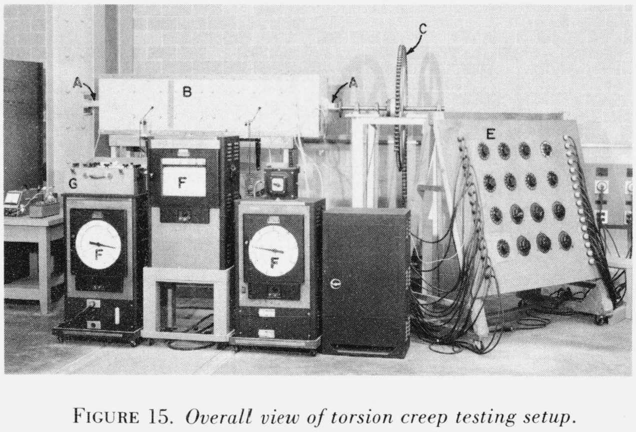

FIGURE 15. *Overall view of torsion creep testing setup.*

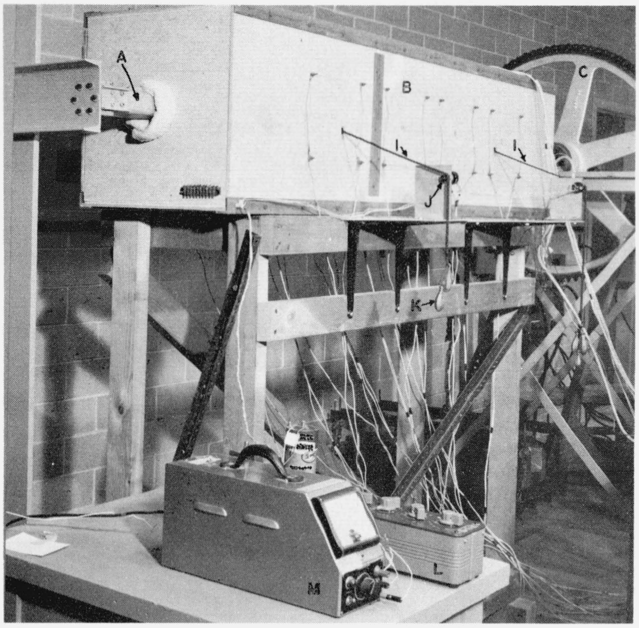

FIGURE 16. *Torsion creep testing setup.*
View from left side.

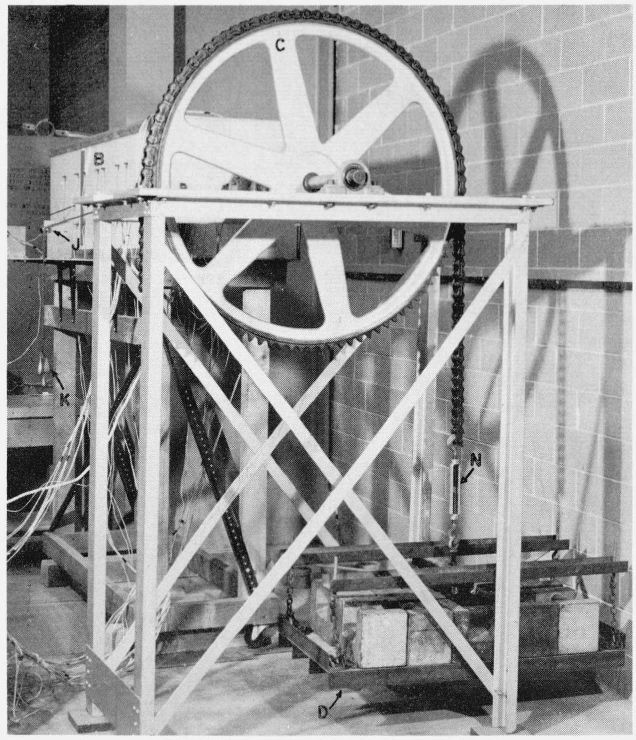

FIGURE 17. *Torsion creep testing setup.*
View from right side.

test specimen by means of a weight pan (D, fig. 17) suspended from the sprocket chain.

The test furnace is fabricated of transite, with steel reinforcement at the edges. The side of the furnace which faces the wall in figure 15 is hinged. Figure 18 is a view of the furnace, in a different location, with the hinged side opened to reveal the interior. Heat is supplied by 32 tubular infrared lamps rated at 120 V and 500 W. The lamps are wired in parallel pairs, the voltage to each pair being adjustable by one of a bank of variable autotransformers (E, fig. 15). Power is regulated by three time-proportioning, potentiometer-type temperature controllers (F, fig. 15), each controlling the temperature over approximately one-third of the furnace. Nine chromel-alumel thermocouples were spot welded to the outer surface of each torsion specimen, at various locations within the three-foot gage length. Three of these thermocouples served as the sensors for the temperature controllers and their outputs were continuously recorded. Outputs of the other six thermocouples were monitored with a calibrated millivolt potentiometer (G, fig. 15), which was also used to periodically check the calibration of the temperature recorders.

Thermocouples cannot normally be spot welded to the structural aluminum alloys with portable, laboratory-type spot welding apparatus. However, the usual alternative mounting technique, clamping, was considered to be particularly undesirable for this type of specimen since the clamps would have to be large as well as numerous and, therefore, deleterious to the attainment of a uniform temperature distribution. Hence, a new technique was devised for spot welding thermocouple beads to 2024-T3 aluminum alloy, which turned out to be completely successful. The technique, in brief, consists of spot welding a small piece of 0.004-in gold foil, about 1 mm square, to the aluminum and then spot welding the thermocouple bead to the foil.

Twist was measured with a troptometer [6] developed specifically for this investigation. Steel sprockets (H, fig. 18) having a pitch diameter of 5.73 in were concentrically attached to the specimen at each end of the three-foot gage length. Sprocket chains (I, figs. 16 and 18) passed over these sprockets and out of the furnace through small holes and thence over a pair of small sprockets (J, figs. 16 and 17) having a pitch diameter of 0.81 in. Each small sprocket is mounted on the shaft of a precision, one-turn, resistance potentiometer rated at 10,000 $\Omega \pm 1$ percent with a linearity tolerance of ± 0.50 percent. The ends of the chains are weighted (K, figs. 16 and 17) to keep them taut.

Torsion of the specimen causes rotation of the 5.73-in sprockets mounted on it. This rotation is transferred, by means of the sprocket chains, to the resistance potentiometers, and magnified by the sprocket ratio. The difference in rotation of the two 5.73-in sprockets, measured as the difference in resistance between the two potentiometers, is the angle of rotation of the specimen over the three-foot gage

[6] trŏp.tŏm'ē.tẽr, n. An instrument for measuring the angular distortion of a bar or piece undergoing a torsion test (Webster). From the Greek *tropos*, turn and *metron*, measure. This word is clearly preferable to any of the existing words used for this purpose in the current literature.

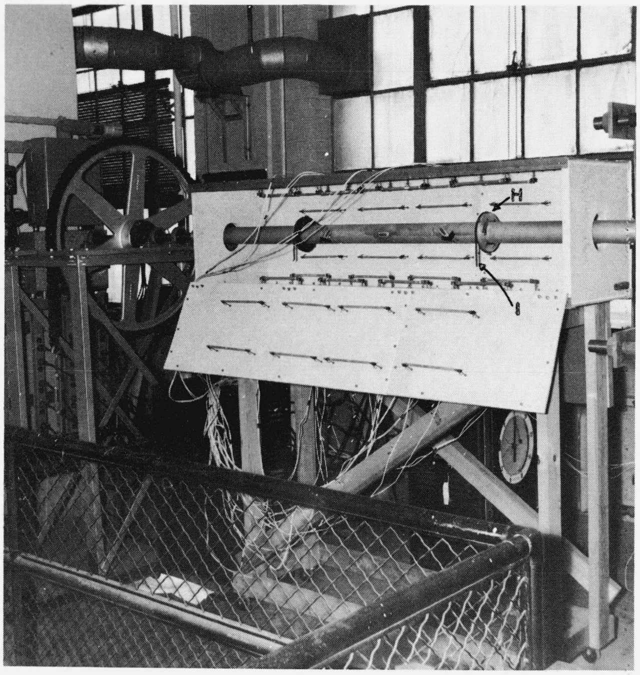

FIGURE 18. *Torsion creep testing setup in a different location with furnace door open.*

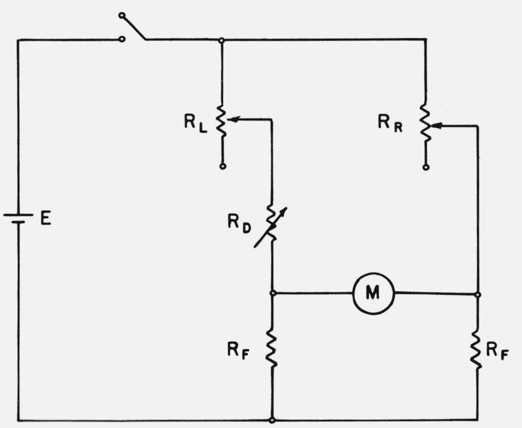

FIGURE 19. *Troptometer bridge circuit.*
E. Dry cell, $1\frac{1}{2}$ V.
M. Null indicator, Honeywell 104 W1G.
R_D. Decade resistance box, 0 to 11,110 Ω.
R_F. Precision fixed resistor, 5,000 Ω.
R_L. Left potentiometer, 0 to 10,000 Ω.
R_R. Right potentiometer, 0 to 10,000 Ω.

length. A bridge circuit, figure 19, is used to measure the difference in resistance between the left and right potentiometers. The decade resistance box (L, fig. 16 and R_D, fig. 19) is periodically adjusted to give a null indication on the meter (M, figs. 16 and 19) and the box setting is then equal to the desired resistance difference. The sensitivity of the null indicator is equivalent to a fraction of an ohm and resistance measurements were made to the nearest ohm. With the sprocket ratios and potentiometers used, one ohm corresponds to an angle of twist of 2.42×10^{-6} radians per inch.

Since an exact solution is available for elastic torsion of circular tubes, a torsion test of a circular tube specimen was carried out at room temperature, within the elastic range, to verify the loading and twist measuring systems. The shear modulus derived from this test was 3.98×10^6 lb/in^2 which agrees with the nominal value of 4.0×10^6 lb/in^2 for 2024-T3 aluminum alloy.

C.2. Procedure

Twelve torsion creep tests were carried out at 400 °F, three on each of the four tube shapes shown in figure 1.

Alinement of each specimen was visually achieved by adjusting the positions of the bearings which support the torque shaft. (This procedure was verified with one 0.083-in wall square tube specimen using resistance strain gages. Thirteen gages were cemented onto the outer surface of the specimen, at various locations, in the longitudinal direction. Torques were applied, within the elastic range, at room temperature. The strain measurements did not reveal the presence of any significant bending or axial force in the specimen.) The weight pan was supported on a platform such that the sprocket chain was unloaded, and weights of the desired amount were stacked upon it. Specimens were heated to the test temperature, 400 °F, in approximately 1 hr, and were kept at this temperature for another hour to permit temperatures to equalize prior to the start of the creep test. The test was started by smoothly raising the weight pan from its platform with a turnbuckle (N, fig. 17) and then removing the platform.

Twist and temperature measurements were made at closely spaced intervals following the start of a test and less frequently thereafter. Twist readings were found to be repeatable within 1 Ω on the decade box (which is equivalent to an angle of twist of less than 3×10^{-6} radians per inch) and temperatures were constant within 1 °F throughout the tests and uniform within 3 °F.

Tests were terminated after approximately 50 hr.

Appendix D. Anisotropic Torsion Creep Theory for Noncircular Tubes

Effects of anisotropy in plastic deformation are commonly included by using a modified expression for the octahedral shear stress, such as

$$\overline{\tau} = \frac{1}{3}\left[\zeta_1(\sigma_x - \sigma_y)^2 + \zeta_2(\sigma_y - \sigma_z)^2 + \zeta_3(\sigma_z - \sigma_x)^2 + 6\zeta_4\tau_{xy}^2 + 6\zeta_5\tau_{yz}^2 + 6\zeta_6\tau_{zx}^2\right]^{1/2} \qquad \text{(D.1)}$$

where x, y, and z are Cartesian coordinates which denote the principal axes of orthotropy and ζ_i are constants. Coordinate x is parallel to the longitudinal axis of the tube. In this form $\bar{\tau}$ does not have physical significance as the shear stress on the octahedral plane unless all the ζ_i are unity; it is simply a measure of the propensity for plastic flow (in this case creep). The octahedral shear creep strain is, as usual,

$$\bar{\gamma}=\frac{2}{3}\left[(\epsilon_x-\epsilon_y)^2+(\epsilon_y-\epsilon_z)^2+(\epsilon_z-\epsilon_x)^2\right.$$

$$\left.+\frac{3}{2}\gamma_{xy}^2+\frac{3}{2}\gamma_{yz}^2+\frac{3}{2}\gamma_{zx}^2\right]^{1/2}. \qquad \text{(D.2)}$$

Using eqs (D.1) and (D.2) it may be seen that in uniaxial tension with $\sigma_x=\sigma$ and $\epsilon_x=\epsilon$, and assuming Poisson's ratio is one-half,

$$\bar{\tau}=\frac{\sqrt{\zeta_1+\zeta_3}}{3}\,\sigma \text{ and } \bar{\gamma}=\sqrt{2}\epsilon. \qquad \text{(D.3)}$$

Similarly, for pure shear with $\tau_{xy}=\tau$ and $\gamma_{xy}=\gamma$

$$\bar{\tau}=\sqrt{\frac{2\zeta_4}{3}}\,\tau \text{ and } \bar{\gamma}=\sqrt{\frac{2}{3}}\,\gamma \qquad \text{(D.4)}$$

Solving eqs (D.3) and (D.4) simultaneously and substituting eqs (1) and (3) therein gives

$$\gamma=\sqrt{3}k\left(\frac{\sqrt{3}}{2}\frac{ZT}{Ah}\right)^m t^n$$

where

$$Z=\sqrt{\frac{2\zeta_4}{\zeta_1+\zeta_3}} \text{ is the anisotropy parameter.}$$

Performing a contour integration to evaluate γ_m and substituting into eq (2) gives, for a tube of uniform wall thickness

$$\theta=\frac{\sqrt{3}}{2}\frac{P}{A}k\left(\frac{\sqrt{3}}{2}\frac{ZT}{Ah}\right)^m t^n.$$

When $Z=1$, this agrees with the isotropic twist equation, eq (7), and when $Z=1.15$ it agrees with the anisotropic version, eq (10).

(Paper 71C3–256)